Role of buoyancy in the onset of dendritic growth in thin layer electrodeposition

M. Rosso,[1] E. Chassaing,[2] and J.-N. Chazalviel[1]
[1]*Laboratoire de Physique de la Matière Condensée, CNRS, Ecole Polytechnique, 91128 Palaiseau Cedex, France*
[2]*Centre d'Etudes de Chimie Métallurgique, CNRS, 15 Rue Georges Urbain, 94407 Vitry-sur-Seine Cedex, France*
(Received 15 July 1998)

Even in thin, quasi-two-dimensional horizontal cells, electrodeposition of treelike metal aggregates is accompanied by a gravity-induced fluid flow at the electrodes. This convective motion mixes the electrolyte and tends to homogenize the concentration. This results in delaying the time at which the branched aggregates start growing, which roughly coincides with the Sand's time τ at which the concentration goes to zero at the cathode. The relative influence of diffusion and convection on the concentration distributions depends on cell thickness, salt concentration, and current density: depending on these parameters, we predict three different regimes for the onset of dendritic growth. We report here on the experimental observation of these regimes. Our theoretical predictions quantitatively account for the observed behaviors. [S1063-651X(99)01703-1]

PACS number(s): 81.15.Pq, 82.45.+z, 47.20.Bp, 61.43.Hv

I. INTRODUCTION

Recent studies [1–22] have permitted a better understanding of the formation of branched metal aggregates that are often found in electrodeposition from binary electrolytes. In particular, the respective roles of the space-charge-induced local electric fields [2], electroconvection [7,15], and buoyancy-induced convective motion [11–16] have been described in detail. Very recently, de Bruyn has investigated different aspects of the early stages of the electrodeposition [19,21]. One of the results of this very detailed study was the observation of a large and systematic increase of the Sand's time: at this time, in a cell operated in galvanostatic conditions, the concentration goes to zero at the cathode and the cell potential diverges [23].

The aim of this paper is to give an explanation to this phenomenon, based on our previous work on gravity-induced convection [20]. The basic idea is that convective motion mixes the electrolyte and tends to homogenize the concentration. This results in delaying the time when the concentration goes to zero at the cathode.

We will first use the results of our theoretical description of convective motion to calculate the Sand's time in different situations, where either diffusion or convection has a dominant role (Sec. II). Then we will compare our calculation to experiments performed in cells with dimensions allowing us to observe these same situations (Sec. III).

II. THEORETICAL BACKGROUND

Several authors have shown that the growth of branched aggregates starts when the electrolyte concentration goes to zero at the cathode [5,8,9,13,21,22]. In the simple case of a binary electrolyte with no convection, this occurs at the Sand's time τ given by [23]

$$\tau = \pi e^2 D (1+\mu_c/\mu_a)^2 C_0^2/(4J^2). \tag{1}$$

D is the ambipolar diffusion constant for the salt: $D=(D_c\mu_a+D_a\mu_c)/(\mu_a+\mu_c)$, where D_a and D_c, μ_a and μ_c are the anion and cation diffusion constants and mobilities, respectively. C_0 is the initial equivalent salt concentration: $C_0=z_cC_c=z_aC_a$, where C_c and C_a, z_c and z_a are the concentrations and charge numbers of the cations and the anions, respectively. J is the current density.

Convective motion mixes the electrolyte and tends to homogenize the concentration. This results in delaying the time τ_{eff} when the concentration goes to zero at the cathode. We will show how this is related to the occurrence of the different diffusion-convection regimes that we described in Ref. [20].

Typically, after applying the polarization to the cell, one finds three different regimes [20]. First, very soon after the current has been switched on in the cell, one observes the formation of a depleted region at the cathode: this is a normal diffusive regime, where convection is negligible (regime 1). Then, due to density gradients induced by the concentration changes at the electrodes, convection starts at both electrodes, widening the perturbed zone in these regions. When convection becomes the dominant mechanism, fluids with different densities behave approximately as immiscible liquids (regime 2). Finally, at longer times, fluid motion is sufficiently slow that diffusion tends to equalize the concentrations vertically (i.e., along the direction normal to the cell) (regime 3). In this last regime (which we call the diffusion-hindered spreading regime [20]), the extent of the perturbed zone near the electrodes varies as $t^{1/2}$. This behavior is similar to a normal diffusive regime, but with an enhanced diffusion constant D_{eff} [18,20]:

$$D_{\text{eff}} \sim (v d^2/D)^2/(d^2/D) = v^2 d^2/D, \tag{2}$$

where v is the fluid velocity and d is the cell thickness. For typical experimental conditions, D_{eff} can be one order of magnitude larger than the ''normal'' diffusion constant D [20].

Now, depending on experimental conditions, the time τ_{eff} when the concentration goes to zero at the cathode may fall into one of the above three regimes. If τ_{eff} occurs in regime 1, one has the normal Sand's behavior, and $\tau_{\text{eff}}=\tau$. If τ_{eff} occurs in regimes 2 or 3, due to concentration mixing, the Sand's time should be increased. Indeed, Argoul *et al.* and

 ©1999 The American Physical Society

de Bruyn [18,21] have reported that, in their experimental conditions, the cell potential increases at an effective Sand's time, which is one order of magnitude larger than the ''normal'' Sand's time.

In the following, based on the model presented in Ref. [20], we present a theoretical estimate of the effective Sand's time in the presence of buoyancy-induced motion, in the regimes 2 and 3 mentioned above.

We start from the expression we derived in Ref. [20] for the length L of the perturbed region in the vicinity of the electrodes; in regime 2,

$$L \sim \left(\frac{g}{\eta} M v_a C_0\right)^{3/10} d^{3/5} D^{1/5} t^{4/5}, \tag{3}$$

and in regime 3,

$$L \approx 0.222 \left(\frac{g}{\eta} M v_a C_0\right)^{1/3} \frac{d^{4/3}}{D^{1/6}} t^{1/2}. \tag{4}$$

Here, η is the dynamic viscosity of the electrolyte, g is the acceleration of gravity, and $M = d\rho/dC = \text{const}$. M is approximately the mass per unit charge of the salt molecule (for $CuSO_4$, M is approximately one-half of the molecular mass). Finally, $v_a = -\mu_a E$ is the anion migration velocity in the applied electric field E [1,2]. Note that, in regime 1, L is the usual diffusion length, which may be written as

$$L \approx (4Dt)^{1/2}. \tag{5}$$

Now Eq. (3) tells us that L follows a power law behavior as a function of time, and as a function of the different parameters characterizing the cell, but our model could not predict the prefactor k of this power law. From our experiments, we estimated this prefactor to be roughly equal to 0.5 [note, however, that as mentioned in [20], in regime 2, our experimental results for L did not fit perfectly the relation given by Eq. (3)].

Figure 5 of Ref. [20] schematically described the evolution of our system through the different regimes. There is also a fourth regime, which is dominated by the migration of the anions, which triggers the growth of a ramified deposit: this regime will not be considered in the following. Transitions between regimes 1, 2, and 3 are generally expected, at times that we will call in the following t_{co1} (regime 1→regime 2) and t_{co2} (regime 2→regime 3). Note that t_{co1} and t_{co2} correspond, respectively, to times t_1 and t_2 of Ref. [20]. Of course, times t_{co1} and t_{co2} can only be observed if the concentration does not go to zero before, in other words, if $\tau_{\text{eff}} > t_{co1}$ and $\tau_{\text{eff}} > t_{co2}$, respectively.

The expressions for the crossover times can be obtained by equating Eqs. (5) and (3) for time t_{co1}, and Eqs. (3) and (4) for time t_{co2}. We then obtain

$$t_{co1} \approx (2/k)^{10/3} (\eta/gMC_0 v_a)(D/d^2), \tag{6}$$

$$t_{co2} \approx (0.22/k)^{10/3} (\eta/gMC_0 v_a)^{-1/9} (d^2/D)^{11/9}. \tag{7}$$

The anionic velocity v_a may be expressed as a function of the applied current density J [1,2]:

$$v_a = J/C_0 e(1+\mu_c/\mu_a). \tag{8}$$

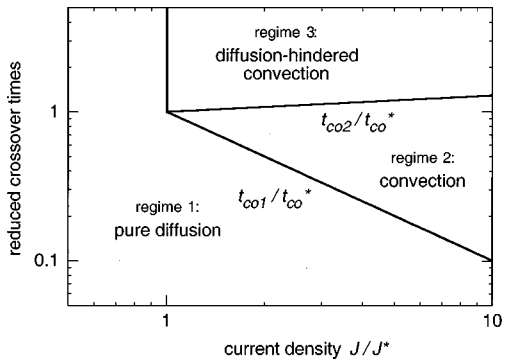

FIG. 1. Schematic diagram showing the three different mass transport regimes and the crossover times t_{co1} and t_{co2} (logarithmic scale). At high current density ($J > J^*$), one finds $t_{co1} < t_{co2}$, a situation which is compatible with the assumption that regime 1 should be observed before regime 2, and regime 2 before regime 3. On the other hand, at low current density ($J < J^*$), Eqs. (9) and (10) imply that $t_{co2} < t_{co1}$, which is in contradiction with the above assumptions (see text). The vertical line separates the two regions $J < J^*$ and $J > J^*$.

From Eqs. (6)–(8) one can calculate the variations of t_{co1} and t_{co2} with J,

$$t_{co1} \approx (2/k)^{10/3} (\eta/gM)[e(1+\mu_c/\mu_a)/J](D/d^2), \tag{9}$$

$$t_{co2} \approx (0.22/k)^{10/3} [(\eta/gM) e(1+\mu_c/\mu_a)/J]^{-1/9} (d^2/D)^{11/9}. \tag{10}$$

A typical result is shown in Fig. 1. The crossover times t_{co1} and t_{co2} follow power laws as a function of J. As the exponents of these power laws are different, there must be a value J^* for which $t_{co1} = t_{co2} = t_{co}^*$. At high current density ($J > J^*$), we have $t_{co1} < t_{co2}$, a situation which is compatible with the assumption that regime 1 should be observed before regime 2, and regime 2 before regime 3.

On the other hand, at low current density ($J < J^*$), one finds $t_{co2} < t_{co1}$, which is in contradiction with the above assumptions. In fact, the times t_{co1} and t_{co2} have no physical meaning here: what actually happens in this case is that the role of convection remains negligible at any time. Hence, the system remains in regime 1 for any $t > 0$.

We now come to the calculation of the effective Sand's time τ_{eff}. We recall that τ_{eff} is the time when concentration goes to zero at the cathode. In regime 1, $\tau_{\text{eff}} = \tau$ [Eq. (1)].

To calculate τ_{eff} in regime 3, we must express the depletion at the cathode, which from [20] may be written as

$$A(0) = C_0 - C(0) \approx 11.0 \left(\frac{g}{\eta} M\right)^{-1/3} (v_a C_0)^{2/3} \frac{D^{1/6}}{d^{4/3}} t^{1/2}, \tag{11}$$

where $C(0)$ is the effective concentration at the cathode. Writing $A(0) = C_0$, one finds for τ_{eff}:

$$\tau_{\text{eff}} = 0.0082 (C_0 Mg/\eta)^{2/3} (d^{8/3}/D^{1/3}) v_a^{-4/3},$$

or, from Eq. (8):

$$\tau_{\text{eff}} = 0.0082 C_0^2 (Mg/\eta)^{2/3} (d^{8/3}/D^{1/3}) [J/e(1+\mu_c/\mu_a)]^{-4/3}. \tag{12}$$

From Eq. (12) we see that τ_{eff} has a $J^{-4/3}$ power-law dependence in regime 3.

Now, in regime 2, the calculation of τ_{eff} is not straightforward because we have no expression for the concentration at the cathode in this regime [20]. In fact, in this regime, we supposed in Ref. [20] that we had two immiscible layers Λ_0 and Λ_1, with concentrations C_0 and $C_1 < C_0$, respectively. The calculation describing regime 2 in Ref. [20] permitted us to determine the thickness $\Delta(x)$ of the layer Λ_1. However, it was only valid in the limit $\Delta(0) \ll d$. To calculate τ_{eff} in regime 2, we will then make a very crude approximation, considering the two-layers system as an average medium, with concentration $C_{\text{av}}(x)$:

$$C_{\text{av}}(x) = (1/d)\{[d - \Delta(x)]C_0 + \Delta(x)C_1\}. \tag{13}$$

Furthermore, we assume $C_1 = 0$. The Sand's time should then correspond to the time when the concentration $C_{\text{av}}(0)$ becomes equal to zero; hence, when $\Delta(0) = d$. To calculate concentration $C_{\text{av}}(0)$, we will assume that

$$[C_{\text{av}}(0) - C_0]\tfrac{3}{4}L \sim C_0 v_a t. \tag{14}$$

This simply derives from the assumption that the concentration depletion near the cathode results from (i) the electrode reaction and (ii) the cationic diffusion toward the cathode. The factor $\frac{3}{4}$ accounts approximately for the shape of the curve $\Delta(x)$ as a function of x. This gives

$$[C_0 - C_{\text{av}}(0)] \approx v_a C_0 (1.33/k)(\eta/gMC_0 v_a)^{3/10} \times d^{-3/5} D^{-1/5} t^{1/5} \tag{15}$$

from which we find

$$\tau_{\text{eff}} = (k^5/4.16)(C_0 Mg/\eta)^{3/2} d^3 D v_a^{-7/2},$$

or, from Eq. (8):

$$\tau_{\text{eff}} = (k^5/4.16) C_0^5 (Mg/\eta)^{3/2} d^3 D [J/e(1 + \mu_c/\mu_a)]^{-7/2}. \tag{16}$$

We show in Fig. 2 the schematic variations (dropping numerical constants) of the different effective Sand's times given by Eqs. (1), (11), and (16) together with the variations of t_{co1} and t_{co2} described in Fig. 1. We find two different situations.

(i) In Fig. 2(a), the line $\tau(J)$ [Eq. (1)] crosses the lines $t_{\text{co1}}(J)$ and $t_{\text{co2}}(J)$ at high J (this corresponds to the region where $t_{\text{co1}} < t_{\text{co2}}$). We then observe four distinct behaviors for the time τ_{eff}. (α) At high J, $\tau(J) < t_{\text{co1}}$: we are in the pure diffusive regime, and we find the classical Sand's behavior described by Eq. (1). The complete depletion at the cathode is attained prior to the onset of convection. (β) At lower J, $\tau(J) > t_{\text{co1}}$: in the pure convective regime, τ_{eff} is now given by Eq. (16). As τ_{eff} varies as $J^{-7/2}$, τ_{eff} becomes larger than τ when J decreases. (γ) At still lower J, $\tau_{\text{eff}} > t_{\text{co2}}$: the system now enters the diffusion hindered regime before complete depletion, and τ_{eff} is given by Eq. (12). Now τ_{eff} varies as $J^{-4/3}$, which increases more slowly than τ when J decreases. (δ) Finally τ_{eff} (regime 3) is equal to τ when J decreases to the value for which $t_{\text{co1}} = t_{\text{co2}}$. Here we find again the system in the pure diffusive regime.

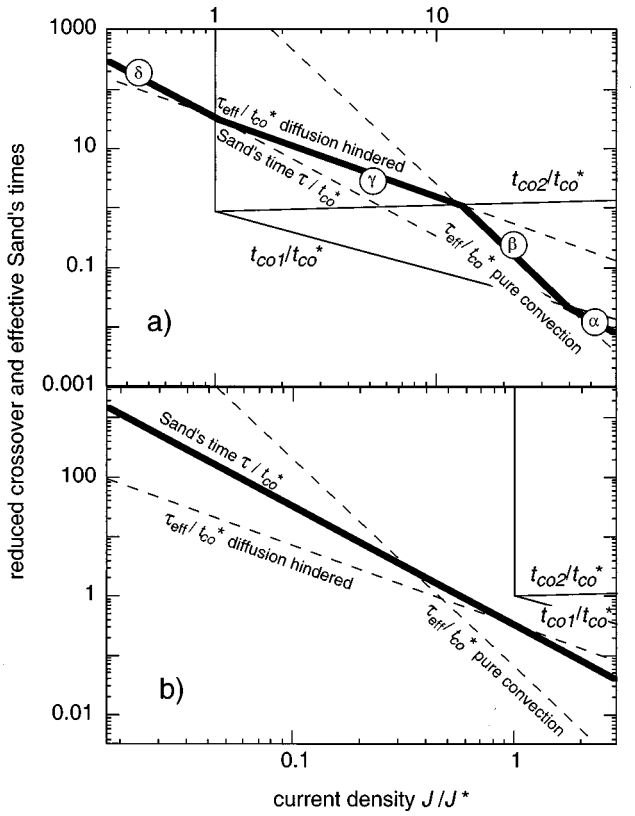

FIG. 2. The thick line shows the variation of the effective Sand's time as a function of the current density J (logarithmic scale). (a) At high concentration and/or cell thickness, one observes four different behaviors for the variation of τ_{eff} with current density J, denoted by letters α, β, γ, and δ (see text). (b) At low concentration and/or cell thickness, convection has no influence on τ_{eff}, and one always observes the normal Sand's behavior described by Eq. (1).

(ii) In Fig. 2(b), the line $\tau(J)$ [Eq. (1)] crosses the lines $t_{\text{co1}}(J)$ and $t_{\text{co2}}(J)$ at low J (this corresponds to the region where $t_{\text{co1}} > t_{\text{co2}}$). One is always in the pure diffusive regime, i.e., the Sand's time follows the classical relation (1). This typically happens at low concentration and/or low cell thickness.

We will now describe an experimental verification of our predictions.

III. EXPERIMENTS

The experimental setup has been described elsewhere in detail [8,13,20]. In the present paper we have studied the electrodeposition of copper from copper sulfate 5×10^{-2} mol l^{-1}, in thin rectangular cells. Two electrolyte layer thicknesses have been used: 0.012 and 0.05 cm. The parallel horizontal plates were made of glass. The copper electrodes were polished with SiC polishing paper (1200 grade). The depositions were performed under constant current, with current densities in the range 1–30 mA cm^{-2}.

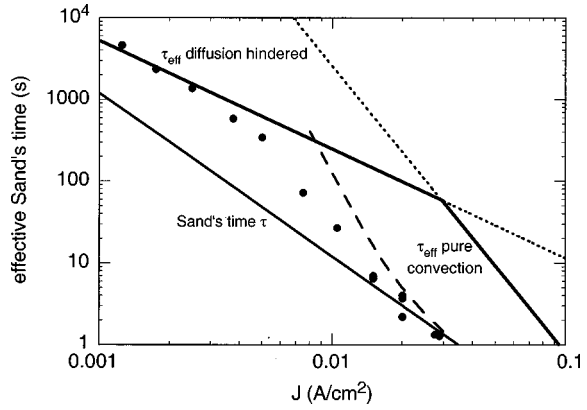

FIG. 3. Variation of the experimental time t_1 (closed circles) as a function of the current density J, compared to the variations of the Sand's time τ and of the effective times τ_{eff} (solid lines, see text). Concentration $C_0/2$ of the electrolyte is 0.05 mol l^{-1}, and cell thickness is 0.05 cm: this corresponds to the situation described in Fig. 2(a). We also show in this figure the results of a corrected calculation for τ_{eff} in the pure convective regime (dashed line, see text).

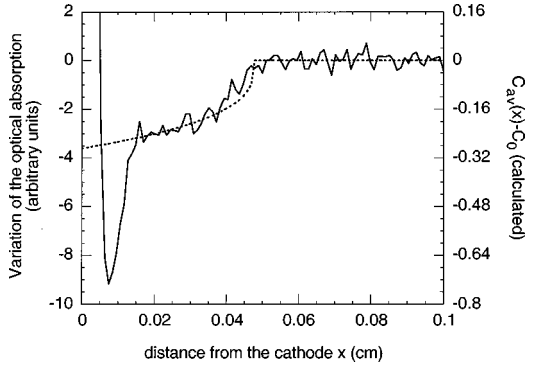

FIG. 4. Comparison of the optical absorption profile in the vicinity of the cathode (solid line) with the concentration profile, calculated according to Eq. (11) and Ref. [20] (dotted line). The experimental data have been recorded 17 seconds after the current has been switched on. Concentration $C_0/2$ of the electrolyte is 0.05 mol l^{-1}, current density is $J=0.02$ A/cm^2, and cell thickness $d=0.05$ cm.

Time evolution of the cell potential $V(t)$ (between anode and cathode) was systematically recorded during the polarizations.

The variation of ionic concentration in the electrolyte was measured from IR light absorption experiments [13], in the vicinity of the cathode. Absorption from Cu^{2+} ions is proportional to concentration: concentration profiles are then directly obtained from these measurements.

In agreement with de Bruyn [21], we found a $V(t)$ curve exhibiting several features. In the following, we will concentrate on the time t_1, corresponding to the largest peak in the dV/dt curve: this peak was found to correspond to the appearance of rough growth on the cathode [21]. Figure 3 shows the variation of time t_1 with the current density J, compared with the time τ_{eff} calculated in Sec. II. The cell thickness is $d=0.05$ cm. This situation corresponds to the case described in Fig. 2(a): we predicted four different behaviors. Due to experimental limitations, we can only observe three of these behaviors, namely, α, β, and γ in Fig. 2(a). Indeed, it is very difficult to perform experiments corresponding to very short times (high J, $\tau_{\text{eff}}<1$ s), or very long times (low J, $\tau_{\text{eff}}>10\,000$ s). For high current densities, the high power dissipated in the cell may induce local temperature increases, whereas for low current densities, it may be difficult to keep the experimental conditions constant during the very long period needed to reach concentration depletion at the cathode.

As mentioned in Sec. II, we have to determine the prefactor k of our pure convective model. We show in Fig. 4 a comparison between the experimental optical absorption profile in the vicinity of the cathode and the concentration profile, calculated according to Eq. (11) and Ref. [20]. Experimental conditions are such that we are in the pure convective regime: the cell thickness is $d=0.05$ cm and the current density is $J=0.02$ A/cm^2. The absorption profile is adjusted, so that it coincides with the concentration profile (remember that optical absorption is proportional to the concentration). The prefactor k is determined by equating the experimental and the calculated lengths of the depleted zone. Here, we find a value $k=0.33$, slightly lower than the value $k=0.46$ mentioned in Ref. [20]. We also observe in Fig. 4 that the theoretical curve correctly fits the experimental data at distances larger than 0.015 cm. Close to the electrode, one observes a negative peak in the concentration profile: This dip is associated with the diffusion layer in the vicinity of the cathode. Such a dip was also obtained from our numerical calculations presented in Ref. [20] which showed that its intensity and width were almost constant in time.

One observes a good agreement between the experimental time t_1 and the calculated time τ_{eff} for behaviors (α) and (γ) (i.e., in the pure diffusive regime, and in the diffusion-hindered regime, respectively). On the other hand, in the pure convective regime [case (β)] the experimental variation observed for t_1 is shifted to the lower time side, in comparison with the calculated τ_{eff}. We attribute this discrepancy to the fact that the ''pure convective regime'' approximation only partially accounts for the convective motion observed in this case; for example, the dip in the concentration profile is not accounted for by this approximation. The existence of this dip has two consequences: (a) the calculation of C_{av} [Eq. (14)] must be corrected to take into account this peak, and (b) the concentration $C_{\text{av}}(0)$ at the cathode is much lower than the value given by Eq. (15); hence, the time τ_{eff} is much lower than the value given by Eq. (16).

The dotted line in Fig. 3 is calculated using the following approximation: we consider the dip in the concentration profile to remain constant after t_{co1}. More precisely, we take its intensity equal to a value $\Delta C=J(4Dt_{\text{co1}}/\pi)^{1/2}/[eD(1+\mu_c/\mu_a)]$ (see Ref. [13]). This results in a slightly more complex determination for τ_{eff}, which we have to calculate numerically. Indeed, we obtain a large decrease in the calculated τ_{eff}, which fits the experimental results much better.

In Fig. 5, we show experimental results similar to those presented in Fig. 3, but for a cell thickness $d=0.012$ cm. This situation now corresponds to the case described in Fig. 2(b): one observes that the time τ_{eff} is very close to the Sand's time τ given by Eq. (1). This confirms our prediction for the case described in Fig. 2(b).

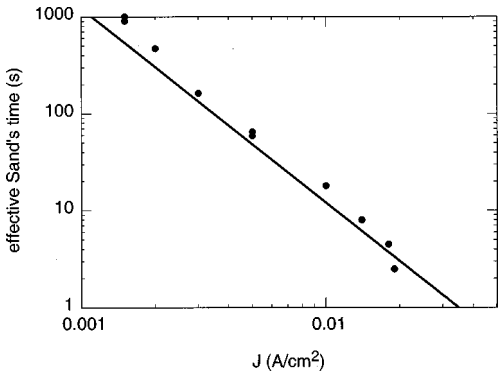

FIG. 5. Variation of the experimental time t_1 (closed circles) as a function of the current density J, compared to the variation of the Sand's time τ (solid line): the concentration is the same as in Fig. 3, the cell thickness is now 0.012 cm. This corresponds to the situation described in Fig. 2(b).

More generally, our results for t_1 are in good agreement with those reported by de Bruyn in Ref. [21]. Hence, we believe that we provide here a quantitative explanation for the increased Sand's time described by this author. This also explains similar results reported in the literature [17].

Finally, one can wonder about the possible influence of electroconvection on the results discussed above. In fact, we believe that there is no influence. Electroconvective motion is due to the motion of the cations in the high electric field, which builds up around the tips of the growing aggregates [6,7]: this electric field is the consequence of the formation of space charges [1]. Now, in principle, no space charges are formed before the onset of ramified growth, which has been shown to occur at the Sand's time [5,8,9,13,21,22]. As a consequence the Sand's time should not be affected by electroconvection, which only starts afterward.

IV. CONCLUSION

We have measured the Sand's time as a function of current density for two different cell thicknesses, corresponding to two distinct situations: for the thinner cell ($d = 0.012$ cm), the perturbation on the concentration at the cathode due to buoyancy driven motion is not sufficient to perturb the Sand's behavior. On the other hand, for the thicker cell, we observe that, in a limited current density range, the Sand's time is enhanced, due to concentration mixing related to convection. Our theoretical results account quantitatively for our experimental results, as well as for data previously reported in the literature.

[1] J.-N. Chazalviel, Phys. Rev. A **42**, 7355 (1990).
[2] V. Fleury, J.-N. Chazalviel, M. Rosso, and B. Sapoval, J. Electroanal. Chem. Interfacial Electrochem. **290**, 249 (1990).
[3] V. Fleury, M. Rosso, and J.-N. Chazalviel, Phys. Rev. A **43**, 6908 (1991).
[4] D. P. Barkey, J. Electrochem. Soc. **138**, 2912 (1991).
[5] V. Fleury, M. Rosso, J.-N. Chazalviel, and B. Sapoval, Phys. Rev. A **44**, 6693 (1991).
[6] V. Fleury, J.-N. Chazalviel, and M. Rosso, Phys. Rev. Lett. **68**, 2492 (1992).
[7] V. Fleury, J.-N. Chazalviel, and M. Rosso, Phys. Rev. E **48**, 1279 (1993).
[8] E. Chassaing, M. Rosso, B. Sapoval, and J.-N. Chazalviel, Electrochim. Acta **38**, 1941 (1993).
[9] F. Argoul and A. Kuhn, J. Electroanal. Chem. **359**, 81 (1993).
[10] A. Kuhn and F. Argoul, Phys. Rev. E **49**, 4298 (1994); J. Electroanal. Chem. **371**, 93 (1994).
[11] D. P. Barkey, D. Watt, Z. Liu, and S. Raber, J. Electrochem. Soc. **141**, 1206 (1994).
[12] C. Livermore and P.-z. Wong, Phys. Rev. Lett. **72**, 3847 (1994).
[13] M. Rosso, J.-N. Chazalviel, V. Fleury, and E. Chassaing, Electrochim. Acta **39**, 507 (1994).
[14] F. Argoul and A. Kuhn, Physica A **213**, 209 (1995).
[15] J. M. Huth, H. L. Swinney, W. D. Mc Cormick, A. Kuhn, and F. Argoul, Phys. Rev. E **51**, 3444 (1995).
[16] K. Linehan and J. R. de Bruyn, Can. J. Phys. **73**, 177 (1995).
[17] M. Z. Bazant, Phys. Rev. E **52**, 1903 (1995).
[18] F. Argoul, E. Freysz, A. Kuhn, C. Léger, and L. Potin, Phys. Rev. E **53**, 1777 (1996).
[19] J. R. de Bruyn, Phys. Rev. E **53**, R5561 (1996).
[20] J.-N. Chazalviel, M. Rosso, E. Chassaing, and V. Fleury, J. Electroanal. Chem. **407**, 61 (1996).
[21] J. R. de Bruyn, Phys. Rev. E **56**, 3326 (1997).
[22] J. Elezgaray, C. Léger, and F. Argoul, J. Electrochem. Soc. **145**, 2016 (1998).
[23] H. J. S. Sand, Philos. Mag. **1**, 45 (1901).